PLATO: verification of in-orbit performances through STOP analysis

Davide Greggio[a], Demetrio Magrin[a], Nicolas Gorius[b], Giovanni Tropea[c], Paolo Apollonio[c], Maria Fuermetz[c], Andrea Cottinelli[a], Duncan Goulty[d], Thomas Kanitz[d], Giacomo Dinuzzi[e], Francesco Santoli[f], Alexander Kuisl[c], Sami-Matias Niemi[d], Isabella Pagano[b], Martin Pertenais[g], and Roberto Ragazzoni[h]

[a]INAF - Osservatorio Astronomico di Padova, Vicolo dell'Osservatorio 5, 35122 Padova, Italy
[b]INAF - Osservatorio Astrofisico di Catania, Via S. Sofia 78, 95123 Catania , Italy
[c]OHB System AG, Manfred-Fuchs-Str. 1, 82234 Weßling, Germany
[d]European Space Agency/ESTEC, Keplerlaan 1, 2201 AZ Noordwijk, The Netherlands
[e]INAF - Osservatorio Astrofisico di Arcetri, Largo Enrico Fermi 5, I-50125, Firenze, Italy
[f]IAPS - INAF Istituto di Astrofisica e Planetologia Spaziali, Via del Fosso del Cavaliere 100, 00133, Roma, Italy
[g]German Aerospace Center (DLR), Institute for Optical Sensor Systems, Rutherfordstr. 2, 12489 Berlin, Germany
[h]INAF - Sede Centrale, Viale del Parco Mellini n.84, 00136 Roma, Italy

ABSTRACT

A STOP (Structural, Thermal, Optical and Performance) analysis has been conducted on the camera units of the PLATO space mission. The analysis is devoted to the prediction of in-orbit performance metrics that could not be otherwise verified through direct testing. The analysis presented in this paper is restricted to the so-called "static cases" which provide a snapshot of a specified thermal condition. These are intended to evaluate the camera performance over the expected operational temperature range and at zero gravity. We hereby provide a description of the model, the requirements to be tested, the simulation strategy and the performance results.

Keywords: space cameras, STOP analysis, optical performance, exoplanets, wide field

1. INTRODUCTION

PLATO (PLAnetary Transits and Oscillations of stars)[1] is the Cosmic Vision Program M3 mission selected by the ESA Science Program Committee (SPC) for launch in 2026 and it will be put into orbit at the Lagrange point L2. The mission aims at detecting and characterizing terrestrial exoplanets orbiting nearby bright stars ($m_V < 13$), with particular interest for solar type stars. The payload is composed of 26 wide field Cameras mounted on a common optical bench and subdivided in 24 "normal type" cameras (N-CAM), dedicated to scientific observations, and two "fast type" cameras (F-CAM), dedicated to the observation of very bright stars ($m_V < 8$) in two different photometric bands (one in blue 505-700nm, and one in red 665-1050nm). Each PLATO Camera is further subdivided into sub-units: 1) the Telescope Optical Unit (TOU) based on a fully refractive optical design[2,3] which includes the light-gathering optics and the baffle; 2) the Focal Plane Array (FPA),[4] which is composed by four CCDs; 3) the Front End Electronics (FEE), that transmits to a corresponding Data Processing Unit[5] and 4)the Camera Thermal Control System (CAM-TCS) made by heaters, sensors, harness and MLI and which is used to precisely control the focusing of the Cameras by acting on thermistors placed along the TOU.[6]

During the various phases from design to production and finally to the delivery of the final product, systematic and controlled procedures have been envisaged to assure that all the deliverables related to the baseline comply

Further author information:
D. Greggio: E-mail: davide.greggio@inaf.it

Space Telescopes and Instrumentation 2024: Optical, Infrared, and Millimeter Wave, edited by Laura E. Coyle, Shuji Matsuura, Marshall D. Perrin, Proc. of SPIE Vol. 13092, 130924E · © 2024 SPIE · 0277-786X · doi: 10.1117/12.3020466

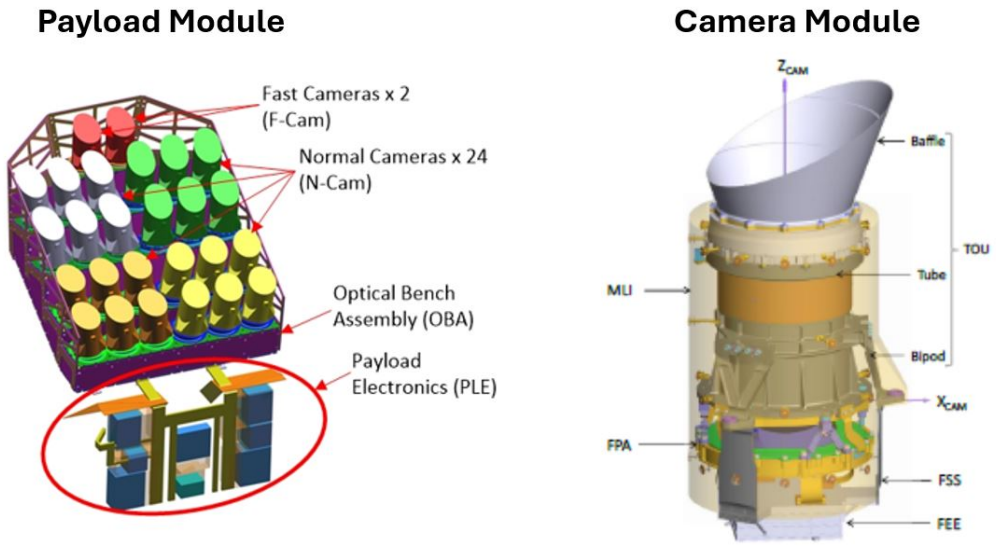

Figure 1. Left: schematic view of the PLATO Payload. Right: 3D view of the Camera Module

with the requirements[7,8] However, some key performance metrics cannot be verified through direct testing of the Camera units. For this reason, a STOP (Structural, Thermal, Optical and Performance) analysis has been conducted, aimed to verify the in-orbit performance of the cameras under a set of observing conditions representative of conservative thermal scenarios. Our analysis focuses on the so-called "Static Cases" (SC), which provide a snapshot of a specified thermal condition and are intended to evaluate the camera performance for that specific thermal environment and at zero gravity. Some further simulations were devoted at analyzing specific conditions useful for comparative studies like the effect of gravity along two perpendicular directions or the simulation of the environment of the test house at the "Institut d'Astrophysique Spatiale" in Paris, in which measurements of the Ensquared Energy (EE) were performed on a real N-CAM model.

In the following sections we provide a brief description of the main requirements to be tested, the model used for the STOP analysis, the simulation strategy and the performance results obtained.

2. REQUIREMENTS TO BE VERIFIED

The requirements that need a verification through the STOP analysis can be divided in three major categories: 1) Functional/operational requirements, 2) Optical performance requirements and 3) Stability requirements. Without entering into the technical details of each requirement, we list them in the following subsections, providing a short description of their target value.

2.1 Functional and operational requirements

- **Operational temperature range**: each camera shall be able to meet the performance requirement during in-orbit operational conditions. The N-CAM and F-CAM shall have the capability to adjust the system focus position by considering a TCS set point temperature between -88°C and -72°C.
- **Operational performance degradations**: performance requirements shall be met during the nominal in-orbit lifetime, considering all environmental effects , tolerances, drifts and degradation.

2.2 Optical performance requirements

- **Ensquared energy in 1x1 pixels**: the brightest pixel flux fraction shall be more than 32% in average across the FoV and less than 80% at every position of the FoV.

- **Ensquared energy in 2x2 pixels**: the Ensquared Energy (EE) of a G0 star PSF in 2x2 pixels shall be higher than 77% in average across the FoV and higher than 70% at every position of the FoV.
- **Ensquared energy in 5x5 pixels**: the Ensquared Energy (EE) of a G0 star PSF in every position of the nominal FoV in 5x5 pixels shall be higher than 99%.

2.3 Stability requirements

- **Boresight stability**: the variation of the camera boresight for a static temperature gradient between any of the bipods at the interface between the Camera and the Optical Bench shall have a sensitivity of less than 1 $arcsec/^{\circ}C$.
- **Entrance pupil area stability**: The entrance pupil area shall have a sensitivity to temperature lower than 40 $ppm/^{\circ}C$.
- **Plate scale stability**: Camera plate scale at the center of FoV shall be 15.0 ± 0.1 $arcsec/px$.

3. SIMULATION STRATEGY

The simulation of thermo-elastic deformations and rigid body motions, and their impact on optical performance, requires the use of several modeling software programs. For our analysis, we used ESATAN-TMS for thermal modeling, Nastran for FEM analysis, and Zemax OpticStudio for optical modeling. Proper communication between these three programs is managed by MultiPAS (Multidisciplinary Software for Structural, Thermal, and Optical Performance Analysis of Space Optical Instruments), developed by OHB Systems AG. Given the complexity of handling all these models, our first step was to verify the final output by simulating a simpler system under uniform temperature conditions. After validating the simulation procedure, we proceeded with the simulation of all the required thermal loads.

For the verification of all the requirements, several "Static Cases" (SC) have been analyzed. The list of all the SC is reported in table 1 and they are subdivided as follows:

- Static cases from SC01 to SC54 have been produced to verify the performance under operational conditions. Depending on the position of the Earth's orbit around the Sun, two different thermal environments have been considered: a "Hot Case" and a "Cold Case".
- SC61 and SC62 are used to assess the impact of gravity along the Z (axial) and X (radial) directions respectively.
- Static cases from SC81 to SC84 are used to verify the requirement about the effect of thermal gradients between the bipods connecting the Cameras to the common Optical Bench.
- Static cases from SC91 to SC94 are used to compare the mathematical model with the measurements taken on the Proto-Flight Model (PFM) at the Institut d'Astrophysique Spatiale test house.
- SC101 is a thermal worst case scenario: all Cameras TRP1 need to be operated at -90°C except for the camera under analysis which is operated at -70°C

Models are defined so that the best focus temperature of the Camera correspond to different set-point temperatures of the TCS as indicated by the TRP-1 value listed in table 1 (see Pertenais, M. et al.[6] for more details on the focusing strategy of the PLATO cameras).

Table 1. List of the executed Static Cases

Case #	Configuration		TRP1	Environment			
	Baffle type	CCD	Temp °C	HC	CC	Test House	Extra
SC01-SC04	Fast	CCD1-4	-80	X			
SC11-SC14	N1/N4	CCD1-4	-80	X			
SC21-SC24	Fast	CCD1-4	-80		X		
SC31-SC34	N1/N4	CCD1-4	-80		X		
SC41	N1/N4	CCD1	-70	X			
SC42			-90	X			
SC43			-70		X		
SC44			-90		X		
SC51	Fast	CCD1	-70	X			
SC52			-90	X			
SC53			-70		X		
SC54			-90		X		
SC61	N1/N4	CCD1	-80	X		X	
SC62	N1/N4	CCD1	-80	X		X	
SC81-SC84	N1/N4	CCD1-4	-80	X			I/F distortion thermal. Worst case with TRP3 and 4 at -80°C and TRP2 at -70°C.
SC91-SC94	N1/N4	CCD1-4	-80			X	PFM @IAS, nominal T°
SC101	N1/N4	CCD1	-70		X		All surrounding CAMs at -90°C

3.1 Input and output models

The input model used for the STOP analysis is based on the PFM "as measured model", which includes measured thicknesses, radii of curvature and refractive indexes, with residual uncertainties. The PFM Camera has also been measured and tested at the Institut d'Astrophysique Spatiale test house, similarly to what was done for the Engineering Model (EM) which was first tested, at the TOU level, at the cryo-vacuum chamber at Leonardo (LDO)[9] and secondly, at the Camera level, at the Netherlands Institute for Space Research (SRON).[10]

The input optical model contains information on the geometry and position of the lenses and the FPA at ambient temperature (T=+20°C) and pressure (P=1 atm). The optical model, combined with the structural model —which includes all the mechanics of the TOU and FPA, including the interface bipods— is then subjected to the steady-state thermal loads representative of each SC. Note that the use of the PFM as the input model allows for the consideration of certain degradation effects, such as alignment and manufacturing tolerances, as required by the "operational performance degradation" specification.

The output model produced by MultiPAS, resulting from the application of thermo-mechanical deformations, is a Zemax OpticStudio file containing the updated geometry and positions of all optical elements. Starting from this file, the temperature of each lens is manually set to the appropriate value obtained from thermal simulations. Additionally, refocusing of the FPA was necessary to align with the Best Image Plane (BIP) at the operating temperature. The offset between the BIP and the FPA position in the output models is attributed to some inaccuracies in modeling the thermal contraction of the FPA module, which prevents full prediction of its final position and cannot be accounted for in the input model preparation. This conclusion is supported by the fact that the obtained offset is consistently $43\mu m$ away from the TOU for all simulated SC with TRP-1 = -80°C, indicating that the defocus is quite insensitive to variations in thermal gradients or gravity deformations. Moreover, the refocus to BIP for the TRP-1=-70°C is $158\mu m$ away from the TOU, while for the TRP-1=-90°C it is $57\mu m$ towards the TOU. Taking the difference between the two and dividing by the temperature difference ($\Delta T = 20°C$), we get a thermal focus sensitivity of $11\mu m/°C$, which matches the value measured on the actual

camera.

After applying the temperature and focus adjustments, the output optical models are ready for the evaluation of all the performance criteria specified by the requirements.

4. PERFORMANCE ANALYSIS AND RESULTS

4.1 Enquared energy analysis

The first performance analysis is devoted to the evaluation of the image quality in terms of ensquared energy for a polychromatic point source. There are requirements about the EE enclosed in 1x1, 2x2 and 5x5 pixels. For all of them we calculate the Huygens PSF for a polychromatic point source. We use a set of eleven wavelengths between 500nm and 1000nm, suitably weighted to reproduce the spectrum of a G0 star. The PSFs are calculated for 44 field points covering the full FoV and are then analyzed through a python script for the extraction of the EE fraction. The python script also accounts for the charge diffusion spread of the PSF, by convolving the image with a gaussian kernel with $\sigma_x = 0.17$ pixels and $\sigma_y = 0.23$ pixels. The EE normalization window is set to 10x10 pixels.

In figure 2 we present the statistics of the EE fraction within 1x1, 2x2, and 5x5 pixels. The figures are violin plots showing the distribution of EE for all simulated field points for each SC. The horizontal line inside each violin represents the average EE value for that SC, while the horizontal red dashed lines indicate the requirements. The first four violins refer to the input model with a uniform temperature of T = -80°C.

For all other simulation conditions, it appears that the greatest variability in EE is due either to the CCD considered (this variability is due to the characteristics of the PFM input file) or to the TCS set-point temperature, rather than other thermo-mechanical load conditions. Moreover, considering the absolute EE fraction, all SCs comply with the requirements. Therefore, we can conclude that the variations induced by thermo-mechanical loads have almost no impact on image quality, provided that the Camera can be refocused to the BIP with the TCS.

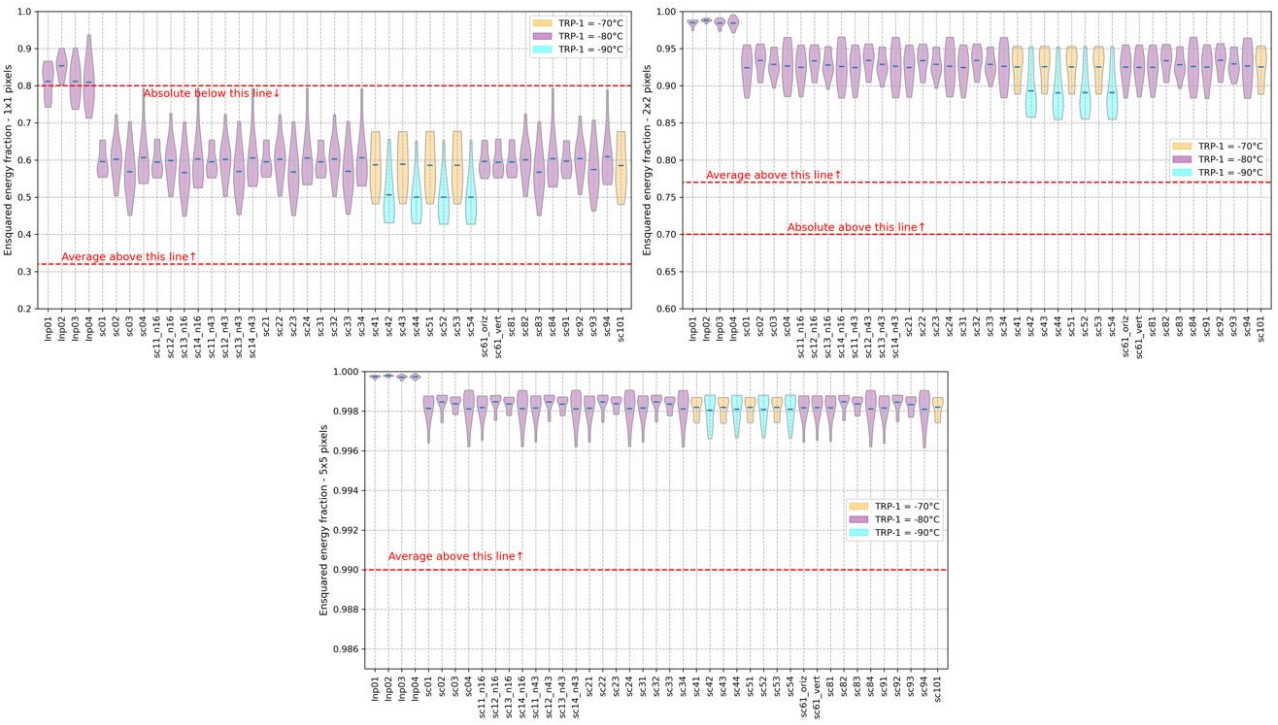

Figure 2. EE fraction within 1x1 pixels (top-left), 2x2 pixels (top-right) and 5x5 pixels (bottom) for all the Static Cases.

4.2 Boresight stability

The boresight variation has been addressed through the static cases from SC81 to SC84 (see table 1 for reference). The thermo-mechanical simulations use the interface between the camera and the Optical Bench (OB) as the static point of the deformations. This means that, from the output model, it is possible to calculate the pointing drift of the single camera, assuming the OB surface is infinitely stable. The pointing variation is evaluated with respect to the reference condition without temperature gradient, corresponding to the static cases SC11-SC14. The pointing is determined by calculating the coordinates of the PSF centroid of the on-axis field. The centroid is calculated through ray-tracing using a 20x20 sampling of the pupil and polychromatic light. As a useful reference, we also calculate the variation of the pointing for the SC61 and SC62, which correspond to the conditions with gravity oriented along the Z and X direction.

The results are reported in table 2. For the cases with gravity, it is estimated that Z-gravity (along the optical axis) has a negligible impact on the pointing, while X-gravity shifts the PSF by $6\mu m$ along the x direction. Being the plate-scale of $1.2\mu m/arcsec$, the shift corresponds to $5arcsec$. The temperature gradient, on the other hand, produces a pointing shift of $3\mu m$ in the x direction, corresponding to $2.5arcsec$ projected on the sky. The simulated gradient between the bipods is 10°C, thus the sensitivity is 0.25arcsec/°C, which is a factor of four smaller than the requirement.

Table 2. pointing variation between SC81-84, SC61-62, and their respective reference cases (SC11-SC14).

SC name	Delta X wrt reference SC [mm]	Delta Y wrt reference SC [mm]
SC61	0.006	0.000
SC62	0.001	0.000
SC81	-0.003	0.000
SC82	-0.003	0.000
SC83	-0.003	0.000
SC84	-0.003	0.000

4.3 Entrance pupil area stability

To verify the requirement, the pupil area is estimated for three SC: 1) SC41 - Load case T=-70°C, 2) SC11 - Load case T=-80°C and 3) SC42 - Load case T=-90°C. For this analysis, the area calculation is performed directly on the mechanical output model, rather than the optical one. The results indicate a sensitivity of 37ppm/°C, which is compliant with the requirement.

4.4 Comparison with test-house measurements

As anticipated in the previous sections, SC91-94 are dedicated to simulate the same thermo-mechanical loads experienced during the EE measurements campaign which took place at the Institut d'Astrophysique Spatiale (IAS) test-house. In this section we provide a comparison between the experimental results and those of the STOP analysis. The measured data are the EE fractions calculated at the best focus temperature from data with exp time 0.3 sec and with a normalization window of 7x7 pixels.

The figures below show the distribution across the field of the EE1x1, EE2x2, EE5x5 for the two data sets. The colormap is the linear interpolation between the available field points. The STOP analysis gives better results compared with the ones measured at IAS even if the average 2x2 EEF differs only by 3%. The distribution over the field is somehow different between the two data sets with a more axially symmetric behaviour of the SC91-94 compared to the IAS measurements. Possible explanations of the differences are biases due to the test setup or lack of information in the STOP models, such as temperature gradients or inhomogeneities inside lenses.

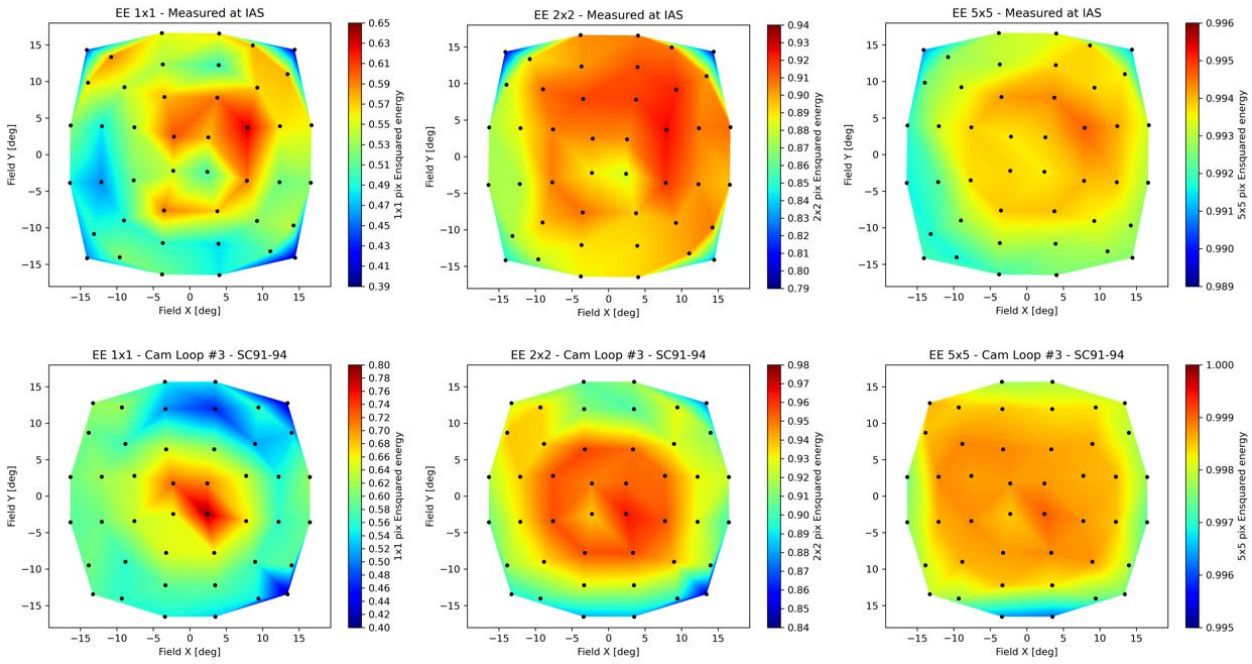

Figure 3. Comparison between the EE fractions measured at IAS (top) and the one obtained from the STOP analysis SC91-SC94 (bottom).

5. CONCLUSIONS

The Structural, Thermal, Optical, and Performance (STOP) analysis conducted on the camera units of the PLATO space mission has provided useful insights into the in-orbit performance, under static thermal conditions. The evaluation of the Ensquared Energy (EE) fractions within 1x1, 2x2, and 5x5 pixels across various field points using a polychromatic point source revealed that the most significant variability in EE is attributed to the characteristics of the input file and to the best-focus working temperature. These factors had a greater impact than other thermo-mechanical load conditions. Despite these variabilities, all camera units (SCs) met the EE requirements. This indicates that thermo-mechanical loads have minimal impact on image quality, provided that each camera can be refocused to the Best Image Plane (BIP) using the TCS.

The analysis addressed boresight variations through static cases SC81 to SC84, using the interface between the camera and the Optical Bench (OB) as the static deformation point. The results indicated that a temperature gradient between the mounting bipods produces a pointing drift of 0.25arcsec/°C, a factor four better than the requirement.

The stability of the entrance pupil area was also evaluated for three static cases (SC41, SC11, and SC42) under different temperature conditions. The results showed a sensitivity of 37 ppm/°C, which is compliant with the requirements.

A comparison between the STOP analysis results and the experimental data from the Institut d'Astrophysique Spatiale (IAS) test-house was performed. The STOP analysis provided better results compared to the IAS measurements, with the average 2x2 EE fraction differing by only 3%. Overall, the STOP analysis confirms that the PLATO camera units meet the required performance metrics under the specified static thermal conditions. The findings indicate that both the thermo-mechanical and optical performance of the camera units are robust, ensuring high image quality and stability in orbit.

ACKNOWLEDGMENTS

DGr, DMa,NGo, ACo, GDi, FSa, IPa, RRa acknowledge support from PLATO ASI-INAF agreement n. 2022-28-HH.0

REFERENCES

[1] Rauer, H., Catala, C., Aerts, C., Appourchaux, T., Benz, W., Brandeker, A., Christensen-Dalsgaard, J., Deleuil, M., Gizon, L., Goupil, M. J., Güdel, M., Janot-Pacheco, E., Mas-Hesse, M., Pagano, I., Piotto, G., Pollacco, D., Santos, Ċ., Smith, A., Suárez, J. C., Szabó, R., Udry, S., Adibekyan, V., Alibert, Y., Almenara, J. M., Amaro-Seoane, P., Eiff, M. A.-v., Asplund, M., Antonello, E., Barnes, S., Baudin, F., Belkacem, K., Bergemann, M., Bihain, G., Birch, A. C., Bonfils, X., Boisse, I., Bonomo, A. S., Borsa, F., Brandão, I. M., Brocato, E., Brun, S., Burleigh, M., Burston, R., Cabrera, J., Cassisi, S., Chaplin, W., Charpinet, S., Chiappini, C., Church, R. P., Csizmadia, S., Cunha, M., Damasso, M., Davies, M. B., Deeg, H. J., Díaz, R. F., Dreizler, S., Dreyer, C., Eggenberger, P., Ehrenreich, D., Eigmüller, P., Erikson, A., Farmer, R., Feltzing, S., de Oliveira Fialho, F., Figueira, P., Forveille, T., Fridlund, M., García, R. A., Giommi, P., Giuffrida, G., Godolt, M., Gomes da Silva, J., Granzer, T., Grenfell, J. L., Grotsch-Noels, A., Günther, E., Haswell, C. A., Hatzes, A. P., Hébrard, G., Hekker, S., Helled, R., Heng, K., Jenkins, J. M., Johansen, A., Khodachenko, M. L., Kislyakova, K. G., Kley, W., Kolb, U., Krivova, N., Kupka, F., Lammer, H., Lanza, A. F., Lebreton, Y., Magrin, D., Marcos-Arenal, P., Marrese, P. M., Marques, J. P., Martins, J., Mathis, S., Mathur, S., Messina, S., Miglio, A., Montalban, J., Montalto, M., Monteiro, M. J. P. F. G., Moradi, H., Moravveji, E., Mordasini, C., Morel, T., Mortier, A., Nascimbeni, V., Nelson, R. P., Nielsen, M. B., Noack, L., Norton, A. J., Ofir, A., Oshagh, M., Ouazzani, R. M., Pápics, P., Parro, V. C., Petit, P., Plez, B., Poretti, E., Quirrenbach, A., Ragazzoni, R., Raimondo, G., Rainer, M., Reese, D. R., Redmer, R., Reffert, S., Rojas-Ayala, B., Roxburgh, I. W., Salmon, S., Santerne, A., Schneider, J., Schou, J., Schuh, S., Schunker, H., Silva-Valio, A., Silvotti, R., Skillen, I., Snellen, I., Sohl, F., Sousa, S. G., Sozzetti, A., Stello, D., Strassmeier, K. G., Švanda, M., Szabó, G. M., Tkachenko, A., Valencia, D., Van Grootel, V., Vauclair, S. D., Ventura, P., Wagner, F. W., Walton, N. A., Weingrill, J., Werner, S. C., Wheatley, P. J., and Zwintz, K., "The PLATO 2.0 mission," *Experimental Astronomy* **38**, 249–330 (Nov. 2014).

[2] Magrin, D., Munari, M., Pagano, I., Piazza, D., Ragazzoni, R., Arcidiacono, C., Basso, S., Dima, M., Farinato, J., Gambicorti, L., Gentile, G., Ghigo, M., Pace, E., Piotto, G., Scuderi, S., Viotto, V., Zima, W., and Catala, C., "PLATO: detailed design of the telescope optical units," in [*Space Telescopes and Instrumentation 2010: Optical, Infrared, and Millimeter Wave*], Oschmann, Jacobus M., J., Clampin, M. C., and MacEwen, H. A., eds., *Society of Photo-Optical Instrumentation Engineers (SPIE) Conference Series* **7731**, 773124 (July 2010).

[3] Munari, M., Magrin, D., Ragazzoni, R., Pagano, I., Viotto, V., Farinato, J., Chinellato, S., Calderone, F., Marafatto, L., Greggio, D., Bergomi, M., Dima, M., Gorius, N., Cessa, V., Molendini, F., Bandy, T., Piazza, D., Benz, W., Brandeker, A., Novi, A., Battistelli, E., Burresi, M., Capuano, E., Grosso, A., Marinai, M., Nebiolo, M., Salatti, M., Rauer, H., Levillain, Y., and Alvarez, J. L., "The PLATO TOU optical design: description, properties, and nominal performances," in [*Space Telescopes and Instrumentation 2022: Optical, Infrared, and Millimeter Wave*], Coyle, L. E., Matsuura, S., and Perrin, M. D., eds., *Society of Photo-Optical Instrumentation Engineers (SPIE) Conference Series* **12180**, 121804I (Aug. 2022).

[4] Moreno, J., Vielba, E., Manjón, A., Motos, A., Vázquez, E., Rodríguez, E., Saez, D., Sengl, M., Fernández, J., Campos, G., Muñoz, D., Mas, M., Balado, A., Ramos, G., Cerruti, C., Pajas, M., Catalán, I., Alcacera, M. A., Valverde, A., Pflueger, P., and Vera, I., "PLATO FPA. focal plane assembly of PLATO instrument," in [*International Conference on Space Optics — ICSO 2018*], Sodnik, Z., Karafolas, N., and Cugny, B., eds., *Society of Photo-Optical Instrumentation Engineers (SPIE) Conference Series* **11180**, 111803N (July 2019).

[5] Cosentino, R., Focardi, M., Galli, E., Steller, M., Del Vecchio Blanco, C., Pezzuto, S., Giusi, G., Di Giorgio, A. M., Biondi, D., Jeszenszky, H., Ottacher, H., Laky, G., Serafini, L., Loidolt, D., Ottensamer, R., Russi, A., Vela Nuñez, M., Luntzer, A., and Kerschbaum, F., "PLATO: the status of the instrument control unit following its critical design review," in [*Space Telescopes and Instrumentation 2022: Optical, Infrared, and Millimeter Wave*], Coyle, L. E., Matsuura, S., and Perrin, M. D., eds., *Society of Photo-Optical Instrumentation Engineers (SPIE) Conference Series* **12180**, 121801B (Aug. 2022).

[6] Pertenais, M., Cabrera, J., Paproth, C., Boerner, A., Grießbach, D., Mogulsky, V., and Rauer, H., "The unique field-of-view and focusing budgets of PLATO," in [*International Conference on Space Optics — ICSO 2020*], Cugny, B., Sodnik, Z., and Karafolas, N., eds., *Society of Photo-Optical Instrumentation Engineers (SPIE) Conference Series* **11852**, 118524Y (June 2021).

[7] Chinellato, S., Postiglione, G., Bandy, T., Battistelli, E., Bergomi, M., Biondi, F., Borsa, F., Calderone, F., Cessa, V., Farinato, J., Greggio, D., Magrin, D., Marafatto, L., Molendini, F., Munari, M., Natalucci, S., Novi, A., Pagano, I., Piazza, D., Ragazzoni, R., Salatti, M., and Viotto, V., "Product assurance for the PLATO Telescope optical unit," in [*Space Telescopes and Instrumentation 2020: Optical, Infrared, and Millimeter Wave*], Lystrup, M. and Perrin, M. D., eds., *Society of Photo-Optical Instrumentation Engineers (SPIE) Conference Series* **11443**, 114434R (Dec. 2020).

[8] Chinellato, S., Auricchio, N., Postiglione, G., Huesler, J., Bandy, T., Battistelli, E., Buonanno, G., Borsa, F., Brandeker, A., Brienza, D., Calderone, F., Cessa, V., Dinuzzi, G., Farinato, J., Ferrero, M., Liaci, R., Magrin, D., Marafatto, L., Munari, M., Nebiolo, M., Novi, A., Pagano, I., Piazza, D., Ragazzoni, R., Salatti, M., Santoli, F., Saverino, A., Simoncini, M., Viotto, V., and Valletti, D., "The TOU of the PLATO mission from a product assurance point of view," in [*Modeling, Systems Engineering, and Project Management for Astronomy X*], Angeli, G. Z. and Dierickx, P., eds., *Society of Photo-Optical Instrumentation Engineers (SPIE) Conference Series* **12187**, 1218711 (Aug. 2022).

[9] Cottinelli, A., Vassallo, D., Farinato, J., Magrin, D., Biondi, F., Royer, P., Ragazzoni, R., Pagano, I., Pagliazzi, M., and Novi, A., "Hartmann data analysis for PLATO TOU EM," in [*Space Telescopes and Instrumentation 2022: Optical, Infrared, and Millimeter Wave*], Coyle, L. E., Matsuura, S., and Perrin, M. D., eds., *Society of Photo-Optical Instrumentation Engineers (SPIE) Conference Series* **12180**, 121804J (Aug. 2022).

[10] Borsa, F., Cottinelli, A., Gorius, N., Arena, C., Vandenbussche, B., Regibo, S., Huygen, R., Royer, P., Pertenais, M., Martin, C., Appourchaux, T., Alvarez, J. L., van Kempen, T. A., Laauwen, W., Pagano, I., and Ragazzoni, R., "PLATO EM first cryogenic vacuum test campaign PSF results," in [*Space Telescopes and Instrumentation 2022: Optical, Infrared, and Millimeter Wave*], Coyle, L. E., Matsuura, S., and Perrin, M. D., eds., *Society of Photo-Optical Instrumentation Engineers (SPIE) Conference Series* **12180**, 121801D (Aug. 2022).